DSF – 28/99
astro – ph/9907421

New results in primordial nucleosynthesis

S. Esposito[a] *, G. Mangano[a], G. Miele[a], and O. Pisanti[a]

[a]Dipartimento di Scienze Fisiche and INFN, Sezione di Napoli,
Pad. 20 Mostra d'Oltremare, I-80125, Naples, Italy

We report the results of a new accurate evaluation of light nuclei yields in primordial nucleosynthesis. The relic densities of ^4He, D and ^7Li have been numerically obtained *via* a new updated version of the standard BBN code.

1. Introduction

Big Bang Nucleosynthesis (BBN) is one of the most powerful tools to study fundamental interactions since light nuclei abundances crucially depend on many elementary particle properties, like the number of *effective* neutrino degrees of freedom, N_ν. At the moment, however, recent data on ^4He mass fraction, Y_4, and Deuterium (D) and ^7Li abundances, $Y_2 \equiv D/H$ and $Y_7 \equiv^7 Li/H$, produced during BBN are controversial, since there are different sets of results, two of them mutually incompatible: $Y_4^{(l)} = 0.234 \pm 0.002 \pm 0.005$ and $Y_4^{(h)} = 0.243 \pm 0.003$ [1], $Y_2^{(l)} = (3.4 \pm 0.3)10^{-5}$ and $Y_2^{(h)} = (1.9 \pm 0.4)10^{-4}$ [2], $Y_7^{(l)} = (1.6 \pm 0.36)10^{-10}$ and $Y_7^{(h)} = (1.73 \pm 0.21)10^{-10}$ [3] (for a brief summary of the experimental situation on primordial abundances see Ref. [4]).

In spite of this discrepancies, which could be of systematic origin, the above results for ^4He data indicate that one is reaching a precision of the order of percent, requiring a similar level for the uncertainties on the theoretical predictions. Besides the corrections to the proton/neutron conversion rates, which fix at the freeze out temperature $\sim 1\ MeV$ the neutron to proton density ratio, the other main source of theoretical uncertainty comes from nuclear rates relevant for nuclei formation. In some cases, these rates are known to well describe the data in a temperature interval which only partially overlaps the one relevant for BBN, $0.01\ MeV \leq T \leq 10\ MeV$. Recent studies [5], however, show that, in particular for the ^4He mass fraction, the effect is at most as large as the one due to the uncertainty on neutron lifetime τ_n, and smaller than 1%. Therefore it is theoretically justified to look for all sources of theoretical uncertainty up to this level of precision.

In a previous paper [6] we performed a thoroughly analysis of all corrections (electromagnetic radiative corrections, finite nucleon mass corrections, plasma effects) to the rates of the processes converting $n \leftrightarrow p$, i.e. $\nu_e\ n \leftrightarrow e^-\ p$, $\overline{\nu}_e\ p \leftrightarrow e^+\ n$ and $n \leftrightarrow e^-\ \overline{\nu}_e\ p$. Here, we report on a following work [7], where we included the above mentioned corrections in a new updated version of the standard BBN code [8]. This new code was used for integrating the set of equation of BBN and obtaining the values of the primordial light nuclei yields. From the comparison of these predictions with the experimental abundances it is possible to get informations on the effective number of neutrinos and the final baryon to photon density ratio, η.

2. Corrections to Born rates

As is well known, the key parameter in determining the primordial ^4He mass fraction is the value of the neutron to proton density ratio at the

*Talk given by G. Mangano at the *6th San Miniato Topical Seminar on 'Neutrino and Astroparticle Physics'*, San Miniato 1999.

freeze-out temperature $T \sim 1\ MeV$, since almost all residual neutrons are captured in ^4He nuclei due to its large binding energy per nucleon. We shortly summarize the kind of corrections which are studied in detail in [6].

The Born rates, obtained in the tree level $V-A$ limit and with infinite nucleon mass have to be corrected to take into account basically three classes of relevant effects:

i) order α radiative corrections. These effects have been extensively studied in literature and can be classified in *outer* factors, involving the nucleon as a whole, and *inner* ones, which instead depend on the details of nucleon internal structure. Actually, other small effects are expected at higher order in α, since the theoretical value of the neutron lifetime is compatible with the experimental one, $\tau_n^{ex} = 886.7 \pm 1.9\ s$ [9], at 4-σ level only. These additional contributions are usually taken into account by eliminating the coupling in front of the reaction rates in favour of τ_n^{ex}.

ii) All Born amplitudes should also be corrected for nucleon finite mass effects. They affect both the weak amplitudes, which should now include the contribution of nucleon weak magnetism, and the allowed phase space. Initial nucleons with finite mass will also have a thermal distribution in the comoving frame, producing a third kind of finite mass correction.

iii) Since all reactions take place in a thermal bath of electron, positron, neutrinos, antineutrinos and photons, thermal-radiative corrections should be also included, which account for the electromagnetic interactions of the in/out particles with the surrounding medium. They can be evaluated in the real time formalism for finite temperature field theory.

After solving the BBN set of equations, one can see that for all nuclides the pure radiative correction provides the dominant contribution, while the finite nucleon mass effects and the thermal-radiative ones almost cancel each other.

The total proton/neutron conversion rates were fitted, in the range $0.01\ MeV \leq T \leq 10\ MeV$, to the following functional forms,

$$\omega_{n\to p}(z) = \frac{1}{\tau_n^{ex}} \exp\left(-q_{np}\ z\right)\ \sum_{l=0}^{13} a_l\ z^{-l}, \qquad (1)$$

$$\omega_{p\to n}(z) = \frac{1}{\tau_n^{ex}} \exp\left(-q_{pn}\ z\right)\ \sum_{l=1}^{13} b_l\ z^{-l}, \qquad (2)$$

where z is the dimensionless inverse photon temperature, $z \equiv m_e/T$ and the values of the parameters can be found in [7]. Note that Eq. (2) is valid only in the range $0.1\ MeV \leq T \leq 10\ MeV$, because $\omega_{p\to n} \sim 0$ for $T < 0.1\ MeV$. The fits have been obtained requiring that the fitting functions differ by less than 0.1% from the numerical values in the considered range.

3. Numerical code

3.1. The Equations of BBN

Denoting with R the universe scale factor, n_B the baryonic density, $\phi_e \equiv \mu_e/T$ the electron chemical potential, and X_i the nuclide number densities, $X_i = n_i/n_B$, the BBN set of equations is a system of coupled differential equations in the previous unknown functions of time. By expanding the equations with respect to ϕ_e and changing the evolution variable to z, after a little algebra one is left with the following $N_{nuc}+1$ equations,

$$\frac{d\hat{h}}{dz} = \left[1 - \widehat{H}(z,\hat{h},X_j)\ G(z,\hat{h},X_j)\right] \frac{3\hat{h}}{z}, \qquad (3)$$

$$\frac{dX_i}{dz} = G(z,\hat{h},X_j)\ \frac{\widehat{\Gamma}_i}{z}, \qquad (4)$$

where we have introduced the dimensionless baryon density, $\hat{h} \equiv n_B/T^3$, Hubble parameter, $\widehat{H} \equiv H/m_e$, and nuclear rates $\widehat{\Gamma}_i \equiv \Gamma_i/m_e$. The function G in Eq.s (3) and (4) is

$$G(z,\hat{h},X_j) = \left[\sum_\alpha (4\hat{\rho}_\alpha - z\frac{\partial\hat{\rho}_\alpha}{\partial z}) + 4\Theta(z_D - z) \times\hat{\rho}_\nu + \frac{3}{2}\ \hat{h}\sum_j X_j\right] \left\{3\left[\sum_\alpha (\hat{\rho}_\alpha + \hat{\mathrm{p}}_\alpha) + \frac{4}{3}\ \Theta(z_D - z)\hat{\rho}_\nu + \hat{h}\sum_j X_j\right]\widehat{H} + \hat{h}\right.$$

Table 1
The predictions on light element abundances obtained with the numerical code for $\eta = 5 \cdot 10^{-10}$

	Y_2	Y_3	Y_4	Y_7
ω_{Tot}	$0.3638{\cdot}10^{-4}$	$0.1175{\cdot}10^{-4}$	0.2446	$0.2814{\cdot}10^{-9}$
ω_B	$0.3727{\cdot}10^{-4}$	$0.1184{\cdot}10^{-4}$	0.2550	$0.2873{\cdot}10^{-9}$

$$\times \sum_j \left(z\Delta\widehat{M}_j + \frac{3}{2} \right) \widehat{\Gamma}_j \Bigg\}^{-1} \quad . \tag{5}$$

In the previous equation $z_D = m_e\,(MeV)/2.3$ is the inverse neutrino decoupling temperature, $\alpha = e, \gamma$, $\widehat{M}_u = M_u/m_e$ and $\Delta\widehat{M}_j = \Delta M_j/m_e = (M_i - A_i M_u)/m_e$ are the dimensionless atomic mass unit and mass excess. We have neglected, in the original system, terms containing the derivatives of chemical potential. The expression of the dimensionless energy densities and pressures, $\hat{\mathrm{p}}_\alpha \equiv \mathrm{p}_\alpha/T^4$ and $\hat{\rho}_\alpha \equiv \rho_\alpha/T^4$, contained in G, were evaluated taking also into account the γ and $e^\pm$ electromagnetic mass renormalization, and fitted as functions of z for their inclusion in the BBN code (see Appendix A of [7]). The previous effect, changing the γ and $e^\pm$ equations of state, modifies the T_ν/T ratio too. However, the difference between the neutrino temperature evaluated with the correct renormalized masses and the one obtained with approximated expressions, $m_\gamma^R \simeq 0$ and $m_e^R \simeq \alpha T^2/m_e$, results to be smaller than 0.01%, a correction that can be neglected at the level of precision we are interested in.

The initial conditions for Eq.s (3) and (4) are given by

$$\hat{h}_{in} = \frac{2\zeta(3)}{\pi^2}\eta_{in} = \frac{11}{4}\,\frac{2\zeta(3)}{\pi^2}\eta, \tag{6}$$

in terms of the final baryon to photon density ratio, η, and

$$X_i(T_{in}) = \frac{g_i}{2}\left(\zeta(3)\sqrt{\frac{8}{\pi}}\right)^{A_i-1} A_i^{\frac{3}{2}} \left(\frac{T_{in}}{M_N}\right)^{\frac{3}{2}(A_i-1)} \times \eta^{A_i-1}\, X_p^{Z_i}\, X_n^{A_i-Z_i}\, \exp\left\{\frac{B_i}{T_{in}}\right\}, \tag{7}$$

which represents the condition of nuclear statistical equilibrium for an arbitrary i-th nuclide, with g_i internal degrees of freedom, Z_i and A_i charge and atomic number, and B_i binding energy. This condition is satisfied with high accuracy at the initial temperature $T_{in} = 10\ MeV$.

3.2. Numerical Method

The numerical problem of solving the set of equations (3) and (4) is *stiff*, because the r.h.s. of (4) results to be a small difference of large numbers. While in the standard code [8] the implicit differentiating method (backward Euler scheme) [10] for writing the r.h.s. of (4) and a Runge-Kutta solver are used, we choose a method belonging to the class of Backward Differentiation Formulas (BDFs) [10], implemented by a NAG routine.

The new code includes all the 88 reactions between the 26 nuclides present in the standard code with the same nuclear rate data, collected and updated in [11]. However, in order to reduce the computation time we used a reduced network, made of 25 reactions between the first 9 nuclides (see Table 1 of Ref. [7]), verifying that this affects the abundances of light nuclei for no more than 0.01 %.

4. Results and conclusions

We report in Table 1 the predictions for $Y_2 = \frac{X_3}{X_2}$, $Y_3 = \frac{X_4}{X_2}$, $Y_4 = \frac{M_6\ X_6}{\sum_j M_j\ X_j}$ and $Y_7 = \frac{X_8}{X_2}$, corresponding to the complete $n \leftrightarrow p$ rates, ω_{Tot}, and to the Born approximation, ω_B. This last quantity denotes the pure Born predictions for $n \leftrightarrow p$ rates without any constant rescaling of coupling to account for the experimental value of neutron lifetime. These values have been obtained for $N_\nu = 3$ and $\eta = 5{\cdot}10^{-10}$. The net effect of the corrections is to allow a smaller number of neutrons to survive till the onset of nucleosynthesis. This ends up in a smaller fraction of elements fixing neutrons with respect to the pure hydrogen.

In Fig. 1 the predictions on Y_4 are shown for

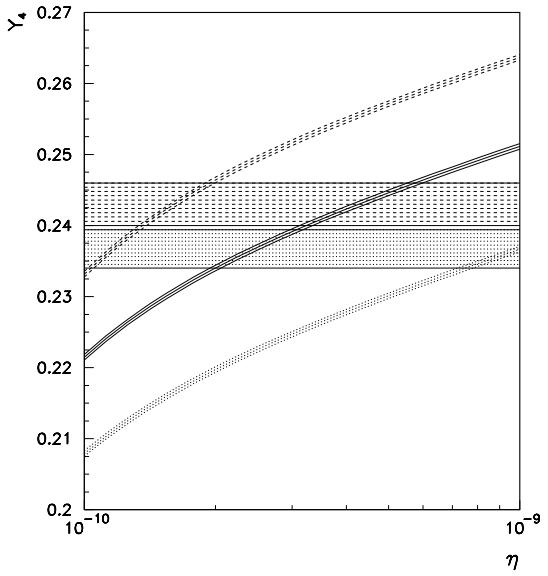

Figure 1. The ^4He mass fraction, Y_4, versus η is shown. The horizontal dashed and dotted bands are the experimental values.

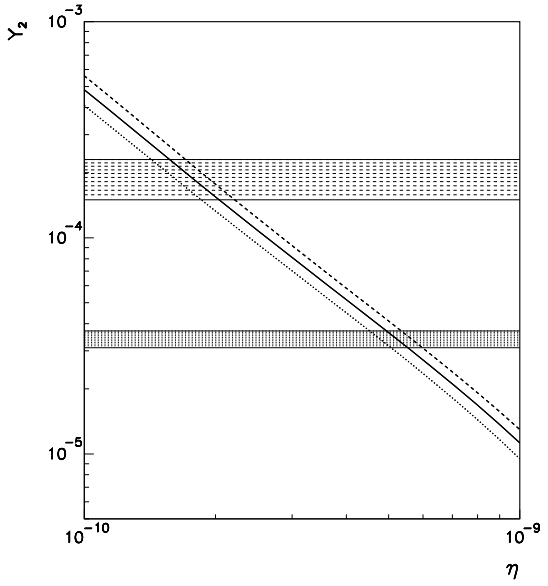

Figure 2. The quantity Y_2 versus η is reported. The horizontal dashed and dotted bands are the experimental values.

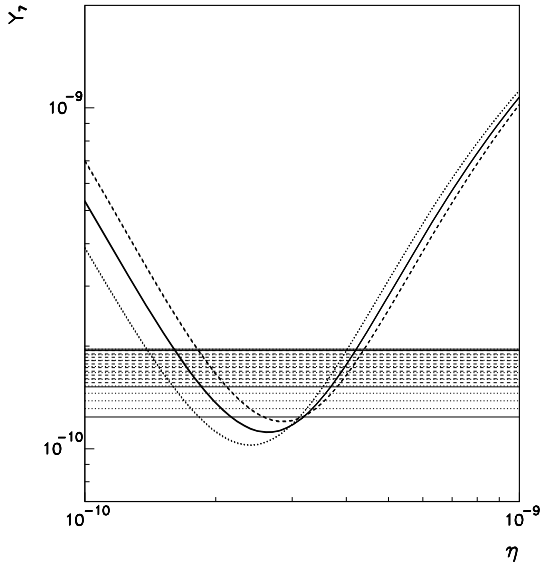

Figure 3. The quantity Y_7 versus η is reported. The horizontal dashed and dotted bands are the experimental values.

$N_\nu = 2, 3, 4$ and for a 1 σ variation of τ_n^{ex}. The three solid lines are, from larger Y_4 to lower values, the predictions corresponding to $N_\nu = 3$ and $\tau_n^{ex} = 888.6\ s$, $886.7\ s$, $884.8\ s$, respectively. Analogously, the dashed lines correspond to $N_\nu = 4$ and the dotted ones to $N_\nu = 2$. The experimental estimates, as horizontal bands, are also reported. In Fig.s 2 and 3 the D and ^7Li abundances are reported with the same notation. Note that, due to the negligible variation of Y_2 and Y_7 on small τ_n changes, no splitting of predictions for 1 σ variation of τ_n^{ex} is present.

By fitting, up to one percent accuracy, Y_2, Y_3, Y_4 and Y_7 as a function of $x = \log_{10}\left(10^{10}\ \eta\right)$, N_ν and τ_n, the following expressions have been obtained:

$$10^3 \cdot Y_2 = \left[\sum_{i=0}^{4} a_i\, x^i + a_5\,(N_\nu - 3)\right] \exp\left\{-a_6\, x + a_7\, x^2\right\}, \qquad (8)$$

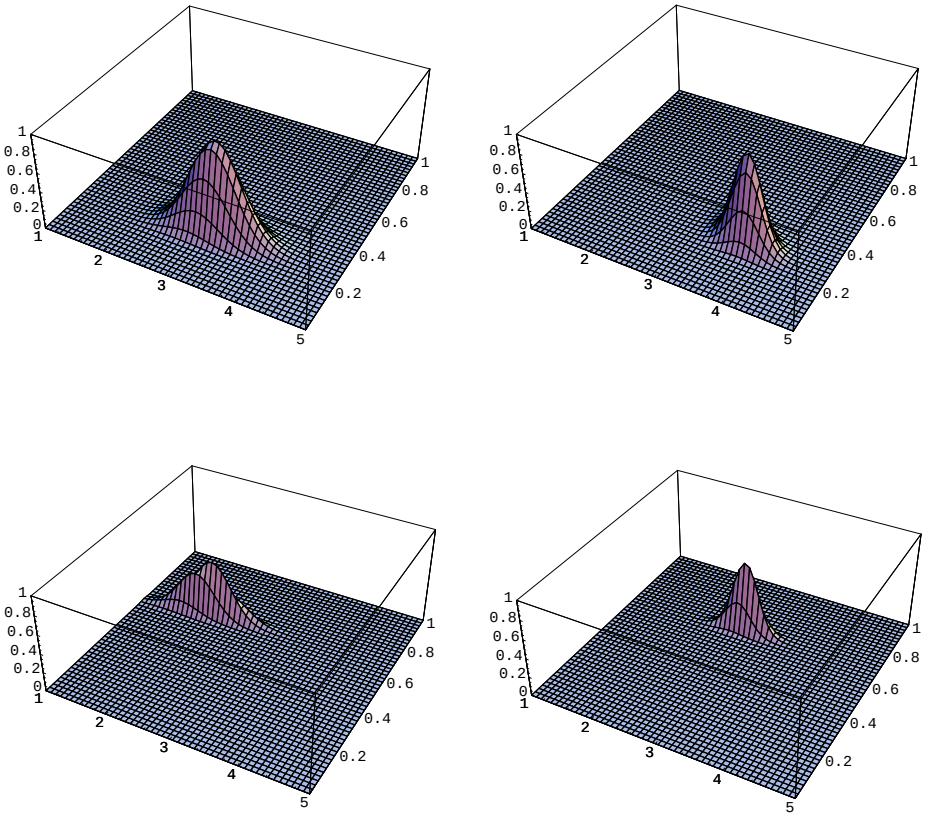

Figure 4. The likelihood distributions for the light element yields Y_2, Y_4, Y_7 are shown as functions of N_ν and $\log_{10} 10^{10}\eta$, in arbitrary units. From left to right and from top to bottom the following cases are considered: a) high D, low ^4He; b) high D, high ^4He; c) low D, low ^4He; d) low D, high ^4He. The normalizations of c) and d) are 25 and 100 times, respectively, the one of a) and b).

$$10^5 \cdot Y_3 = \left[\sum_{i=0}^{4} a_i\, x^i + a_5\,(N_\nu - 3)\right] \exp\{-a_6\, x\}, \quad (9)$$

$$10 \cdot Y_4 = \sum_{i=0}^{5} a_i\, x^i + a_6\,(\tau - \tau_{ex}) + a_7\,(N_\nu - 3) + a_8\, x\,(\tau - \tau_{ex}) + a_9\, x\,(N_\nu - 3), \quad (10)$$

$$10^9 \cdot Y_7 = \left[\sum_{i=0}^{3} a_i\, x^i + a_4\,(N_\nu - 3) + a_5\, x\,(N_\nu - 3)\right] \times \exp\left\{-a_6\, x + a_7\, x^2 + a_8\, x^3 + a_9\, x^4\right\}, \quad (11)$$

where the values of the fit coefficients are reported in Table 3 of [7].

In Fig. 4 we plot the product of gaussian distribution for D, ^4He and ^7Li, centered around the measured values and with their corresponding experimental errors,

$$\begin{aligned} L(N_\nu, x) &= \exp\left(\frac{(Y_2(N_\nu, x) - Y_2^{ex})^2}{2\sigma_2^2}\right) \\ &\times \exp\left(\frac{(Y_4(N_\nu, x) - Y_4^{ex})^2}{2\sigma_4^2}\right) \\ &\times \exp\left(\frac{(Y_7(N_\nu, x) - Y_7^{ex})^2}{2\sigma_7^2}\right). \end{aligned} \quad (12)$$

The experimental values used in the previous equation correspond to the four combinations of experimental results: a) $Y_2^{(h)}$, $Y_4^{(l)}$; b) $Y_2^{(h)}$, $Y_4^{(h)}$; c) $Y_2^{(l)}$, $Y_4^{(l)}$; d) $Y_2^{(l)}$, $Y_4^{(h)}$.

The figure shows that the high value of D is preferred (plots a) and b)). In both cases the distributions are centered in the range $x \in 0.2 \div 0.4$, but at $N_\nu \sim 3$ for low ^4He and $N_\nu \sim 3.5$ for high ^4He. For low D the compatibility with experimental data is worse (note that in c) and d) cases the distributions have been multiplied by a factor of 25 and 100 respectively) and centered in the range $x \in 0.6 \div 0.8$, and at $N_\nu \sim 2$ for low ^4He and $N_\nu \sim 3$ for high ^4He.

REFERENCES

1. B.E.J. Pagel, E.A. Simonson, R.J. Terlevich and M. Edmunds, MNRAS 255 (1992) 325; E. Skillman and R.C. Kennicutt, Astrophys. J. 411 (1993) 655; E. Skillman, R.J. Terlevich, R.C. Kennicutt, D.R. Garnett, and E. Terlevich, Astrophys. J. 431 (1994) 172; Y.I. Izotov, T.X. Thuan, and V.A. Lipovetsky, Astrophys. J. 435 (1994) 647; Astrophys. J. Suppl. 108 (1997) 1.
2. R.F. Carswell, M. Rauch, R.J. Weymann, A.J. Cooke, and J.K. Webb, MNRAS 268 (1994) L1; A. Songaila, L.L. Cowie, C. Hogan, and M. Rugers, Nature 368 (1994) 599; M. Rugers and C.J. Hogan, Astrophys. J. 111 (1996) 2135; R.F. Carswell *et al.*, MNRAS 278 (1996) 518; E.J. Wampler *et al.*, Astron. Astrophys. 316 (1996) 33; J.K. Webb, R.F. Carswell, K.M. Lanzetta, R. Ferlet, M. Lemoine, A. Vidal-Madjar, and D.V. Bowen, Nature 388 (1997) 250; D. Tytler *et al.*, astro-ph/9810217 (1998); D. Tytler, X.-M. Fan, and S. Burles, Nature 381 (1996) 207; S. Burles and D. Tytler, Astrophys. J. 460 (1996) 584.
3. J.A. Thorburn, Astrophys. J. 421 (1994) 318; P. Molaro, F. Primas, and P. Bonifacio, Astron. Astrophys. 295 (1995) L47; P. Bonifacio and P. Molaro, Mon. Not. Roy. Astron. Soc. 285 (1997) 847.
4. S. Sarkar, Proceedings of the Second International Workshop on Dark Matter in Astro- and Particle Physics, Heidelberg, 20-25 July 1998, astro-ph/9903183.
5. L.M. Krauss and P. Romanelli, Astrophys. J. 358 (1990) 47; P.J. Kernan and L.M. Krauss, Phys. Rev. Lett. 72 (1994) 3309; G. Fiorentini, E. Lisi, S. Sarkar, and F.L. Villante, Phys. Rev. D58 (1998) 063506.
6. S. Esposito, G. Mangano, G. Miele, and O. Pisanti, Nucl. Phys. B540 (1999) 3.
7. S. Esposito, G. Mangano, G. Miele, and O. Pisanti, preprint DSF 18/99, astro-ph/9906232.
8. R.V. Wagoner, W.A. Fowler, and F. Hoyle, Astrophys. J. 148 (1967) 3; R.V. Wagoner, Astrophys. J. Suppl. 18 (1969) 247; R.V. Wagoner, Astrophys. J. 179 (1973) 343; L. Kawano, preprint FERMILAB-Pub-88/34-A; preprint FERMILAB-Pub-92/04-A.
9. Particle Data Group, G. Caso *et al.*, Eur. Phys. J. C3 (1998) 1.
10. B.P. Flannery, W.H. Press, S.A. Teukolsky, and W.T. Vetterling, Numerical Recipes in Fortran, Cambridge University Press.

11. For the expressions of the rates see the Web sites *http://www.phy.ornl.gov/astrophysics/data/data.html* or *http://pntpm.ulb.ac.be/Nacre/barre_database.htm*.